Mathematical Study of Impact of Non-signalized Road Crossing on Vehicular Emissions and Fuel Consumption

Raj Kumar Pradhan, Samir Shrestha, Dil Bahadur Gurung

***Abstract*—Emissions from vehicles, particularly automobiles, account for around two-thirds of urban air pollution. The principal pollutants generated by motor vehicles, including carbon monoxide (CO), nitrogen oxides (NOx), hydrocarbons (HC) etc., have negative effects on both human health and the environment. The interaction at intersections, particularly in the context of road crossings involving pedestrians and vehicles, can have several environmental impacts. Intersections often lead to traffic congestion, causing vehicles to idle or move at slower speeds. This, in turn, increases fuel consumption and increases pollutants' emissions. These emissions contribute to air pollution and can have adverse effects on air quality. This paper aims to study the impact of the vehicle-pedestrian interaction at the intersection of the road segment on vehicular emissions and fuel consumption through numerical simulations using the car following models by taking a platoon of vehicles. The amount of vehicular emissions like NOx, CO, HC and fuel consumption are fitted through the available data in the literature by using the method of least squares over time against instantaneous speed. The fitted model is then utilized to estimate the rate of vehicular emissions and fuel consumption per kilometer of different types of vehicle with and without interaction at the non-signalized intersection of the road segment. Furthermore, the average emission and fuel consumption of different types of vehicles are studied and compared with the data in the literature.**

***Index Terms*—Pollutant emissions, fuel consumption, intersection, interaction, pedestrians, car-following models.**

I. Introduction

VEHICLE emissions are usually not very high, but as more vehicles travel on the road, environmental pollution rises up to a significant level. Emissions from vehicles, particularly automobiles, account for around two-thirds of urban air pollution [3]. Although car emissions are generally minimal, however the increasing number of automobiles on the road leads to increased environmental contamination. The transportation sector accounts for approximately 35% of CO, 30% of HC, and 25% of NOx emissions into the atmosphere. These substances have negative impacts on both the environment and human health [4]. Vehicles in big urban areas are estimated to contribute 70% of CO, 50% of HC, 30-40% of NOx, 30% of suspended particulate matter (SPM), and 10% of oxides of sulphur (SO_2) to the city's total pollution burden, with two-wheelers accounting for two-thirds [1]. Vehicle emissions have serious health consequences. They contribute to air pollution, which can cause respiratory and genitourinary problems like asthma, bronchitis, chronic obstructive pulmonary disease, and pneumonia. Major pollutants generated by motor vehicles, such as CO, NOx, HC and SPM are harmful to human health. These emissions can have major consequences for human health and the environment, such as respiratory and cardiovascular disorders. Furthermore, automotive exhaust pollutants have been linked to an increase in rates of low birth weight and acute asthma attacks in children. Even in locations with acceptable air quality, studies conducted around the world repeatedly show that car emissions have a harmful impact on health. Overall, emissions from vehicles harm human health, contributing to a variety of respiratory and other health issues.

The interaction at intersections, particularly in the context of road crossings involving pedestrians and vehicles, can have several environmental impacts. Intersections often lead to traffic congestion, causing vehicles to idle or move at slower speeds. This leads to large amount of fuel consumption and higher emissions of pollutants such as CO_2, NOx, CO, and HC. These emissions contribute to air pollution and can have adverse effects on air quality. Stop-and-go traffic at intersections can increase the overall energy consumption of vehicles. Frequent acceleration and deceleration use more fuel and energy compared to steady-state driving. This, in turn, affects the fuel efficiency and increases the overall environmental impact of transportation. Traffic interactions at intersections often lead to increase the noise levels. The acceleration and braking of vehicles, along with honking and other traffic-related sounds, contribute to noise pollution. Prolonged exposure to high noise levels can have negative effects on both human health and the well-being of wildlife. Intersections often influence the layout of urban and suburban areas. The expansion of roads and intersections can lead to the loss of green spaces, including trees and vegetation, affecting local ecosystems and contributing to biodiversity loss.

Efforts to improve the environmental impact of interactions at intersections may involve better urban planning, the implementation of intelligent transportation systems, promotion of public transit and non-motorized transportation, and the use of green infrastructure to mitigate the negative effects.

Manuscript received May 21, 2024; revised March 14, 2025. This work was supported by the University Grants Commission (UGC) Nepal.

Raj Kumar Pradhan is a Senior Assistant Professor of Mathematics at Khwopa College, Bhaktapur, Nepal (email: rajprdhan63@gmail.com).

Samir Shrestha is an Associate Professor of Mathematics at Department of Mathematics, School of Science, Kathmandu University, Nepal (corresponding author to provide email: samirstha@ku.edu.np).

Dil Bahadur Gurung is a Professor of Mathematics at Department of Mathematics, School of Science, Kathmandu university, Nepal (email: db_gurung@ku.edu.np).

The emission rate of vehicles at an intersection while crossing the road can vary based on several factors. Factors influencing vehicle emissions at intersections include traffic flow, vehicle idling, acceleration, and deceleration. Generally, emissions at intersections can be higher than during steady driving due to frequent stops and starts. Key pollutants emitted by vehicles include CO_2, NOx, CO, SPM, and HC.

The emission rate and fuel consumption are affected [5], [6] by

- Idle Time: The longer a vehicle is idling at an intersection, the more emissions it produces. Idling is often a significant contributor to emissions at intersections.
- Acceleration and Deceleration: Aggressive driving behavior, including rapid acceleration and deceleration, can increase emissions. At intersections, drivers may accelerate quickly to clear the intersection or brake suddenly.
- Traffic Flow: Heavy traffic conditions and congestion can lead to more frequent stops and starts, resulting in increased emissions.
- Vehicle Type and Age: Older vehicles or those with outdated emission control technologies may emit higher levels of pollutants.
- Fuel Type: The type of fuel a vehicle uses can influence emissions. For example, diesel engines tend to emit more NOx than gasoline engines.
- Traffic Signal Timing: Well-designed traffic signal timing can improve traffic flow, reducing idling time and emissions.

Quantifying the exact emission rate at a specific intersection would require detailed traffic and emission modeling, taking into account local factors, vehicle types, and driving patterns. Simulation models and tools like the U.S. Environmental Protection Agency's MOVES (Motor Vehicle Emission Simulator) model are often used for such analyses. It is important to note that efforts to reduce emissions at intersections may involve optimizing traffic signal timings, promoting alternative transportation modes, implementing intelligent transportation systems, and encouraging fuel-efficient and electric vehicles. The normalized HC, CO and NOx emission levels of the seven passenger cars older than model year 2000 were $3.19 \pm 5.04, 14.59 \pm 22.88$ and 2.57 ± 2.12 g/km, respectively. The HC, CO and NOx emission levels of other newer vehicles were $0.02 \pm 0.02, 0.23 \pm 0.29$ and 0.10 ± 0.13 g/km, respectively. All the cars were tested at a speed less than 80 km/h. [11]. To estimate the concentrations of vehicular emissions in a practical setting, generalized functions representing the emissions from the entire mixed traffic flow must be established. Two primary variables are frequently used to represent emission functions: the kind of vehicle and its average driving speed. Vehicle type considers characteristics of the vehicle, such as fuel type, engine type, weight, emission technology, and others, that affect emissions. The operational factors that have a more direct impact on emissions, such as engine speed, gear selection, acceleration, and deceleration rate and frequency, are positively connected with average speed. In regional and national inventories, average-speed functions are frequently employed to quantify vehicular emissions like NOx, HC, and CO from motor vehicles.

II. Pedestrian and Vehicle Models

Appropriate mathematical models of both vehicles and pedestrians are essential for studying and analyzing a traffic system. This section explores the vehicle and pedestrian models employed in our study.

A. Pedestrian model

The manner in which pedestrians traverse roadways is subject to a variety of influences, including age, physical capability, traffic dynamics, and cultural standards. Cultural norms and the presence of pedestrian infrastructure play pivotal roles in shaping pedestrian behavior. Across various geographical locations, the approach towards crossing streets may exhibit a spectrum from confident to vigilant, mirroring prevalent cultural values. Within designated pedestrian zones featuring traffic control measures such as signals or marked pathways, individuals typically adhere to a steady gait, making adaptive maneuvers to negotiate vehicular flow.

Central to modeling pedestrian movement are two principal factors: walking speed and age demographics. Pedestrians are typically categorized into distinct age cohorts, namely younger individuals aged between 20 and 64, and older adults aged 65 and above. Younger adults exhibit an average walking speed ranging from 1.36 m/s to 1.61 m/s when crossing streets, while older adults demonstrate a normal walking speed of 1.14 m/s, increasing to 1.36 m/s during street crossings [10]. Consequently, for our study, the pedestrian walking speed v_{pws} is stochastically chosen from the interval of 1.14 m/s to 1.36 m/s for individuals engaged in normal walking activities, with an additional increment of 0.25 m/s applied during street crossings. However, the pedestrians are assumed to arrive at the curb side at the intersection of the road following the Poisson distribution. They move forward following laws of motion. When pedestrians arrive at the curb side near intersection, they observe the vehicles on the road to calculate the vehicles arriving time and crossing time to cross the road. If the road crossing time is smaller than that of vehicle arriving time at the intersection, they cross the road otherwise they wait at the curb side until all the vehicles cross the intersection. The schematic diagram of the road intersection is shown in Fig. 1.

B. Vehicle model

In urban areas, vehicles must adhere to safety regulations to ensure pedestrian safety and comply with traffic laws. Car-following models, which elucidate how drivers trail behind the lead vehicle, have been the subject of study for over fifty years. The geometric center position of a vehicle is commonly utilized to represent its location. Depending on the distance from the lead vehicle and without considering pedestrians, a vehicle can operate within three distinct driving regimes: free driving, car-following, and emergency braking. In the free driving regime, the vehicle autonomously adjusts to achieve its desired speed. This desired speed, denoted as $v_{\max}$ in the model, is typically determined as the lesser

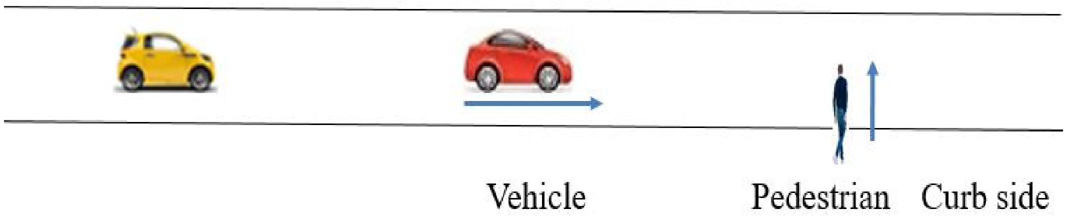

Fig. 1: Schematic diagram of non-signalized road intersection.

value between the legal speed limit and the vehicle's inherent maximum speed. Emergency braking is enacted to avert collisions when the distance between consecutive vehicles falls below a safety threshold, and the following vehicle's speed exceeds that of the lead vehicle.

1) Car-following models: The single-lane car-following model can be modeled as [2], [8], [13]

$$\frac{dv_i}{dt} = f(v_i,\, \Delta x_i,\, \Delta v_i,\, \cdots), \tag{1}$$

where v_i, Δx_i, Δv_i are the speed of i^{th} vehicle, headway and relative speed respectively; f is the stimulus function of i^{th} vehicle. The schematic diagram of car-following model is presented in Fig. 2.

The Optimal Velocity (OV) in a car-following model is introduced by Bando et al. [2]. They defined governing equation as

$$\frac{dx_i}{dt} = v_i\,; \tag{2}$$

$$\frac{dv_i}{dt} = \kappa\{V(\Delta x) - v_i\}, \tag{3}$$

where κ is the reciprocal to the reaction time and the function $V(\Delta x)$ represents the optimal velocity function (OVF). This OVF is determined by the inter-vehicle distance defined as

$$V(\Delta x) = \tanh(\Delta x - 2) + \tanh\, 2 \tag{4}$$

which is assumed monotonically increasing and bounded above function. According to the OV model, each vehicle maintains its top speed while keeping a safe distance from the next one, and a vehicle's optimal velocity is based on how far it is from the next one. The optimal velocity function reflects the tendency of drivers to maintain a safe following distance from the vehicle ahead while also aiming to travel at a desired speed. In many car-following models, the optimal velocity function depends on the difference between the vehicle's current speed and its desired speed. If the vehicle's speed is lower than the desired speed, the optimal velocity function may encourage acceleration. Conversely, if the vehicle's speed exceeds the desired speed, the function may suggest deceleration. The optimal velocity function may also take into account traffic conditions, such as congestion or the speed of surrounding vehicles. For example, in congested traffic, the optimal velocity function might recommend maintaining a slower speed to avoid collisions or sudden stops. Different car-following models may use various formulations for the optimal velocity function. Some models may incorporate driver behavior characteristics, road geometry, or vehicle dynamics to determine the optimal velocity. The specific form of the optimal velocity function can significantly influence the overall behavior of the traffic flow simulated by the model. The OV model is calibrated with respect to empirical data by Helbing and Tilch [7]. They adopted the following optimal function

$$V(\Delta x_i(t)) = V_1 + V_2\, \tanh\left[C_1(\Delta x_i(t) - l_c) - C_2\right], \tag{5}$$

where l_c is considered as the length of the vehicle. The values of parameters are $V_1 = 6.75\, ms^{-1}$, $V_2 = 7.91\, ms^{-1}$, $\kappa = 0.85\, s^{-1}$, $C_1 = 0.13\, m^{-1}$ and $C_2 = 1.57$. When compared to actual field data, it is shown that the OV model had problems with unrealistic deceleration and excessive acceleration. To address this issue, Helbing and Tilch [7] put forward a new model as a solution called Generalized Force Model (GFM) and given by

$$\frac{dv_i(t)}{dt} = \kappa\{V(\Delta x_i(t)) - v_i\} + \lambda\, \Theta(-\Delta v)\, \Delta v, \tag{6}$$

where Θ is the Heaviside function. Θ is one when the leading vehicle of it has velocity lower than that of the following vehicle; otherwise, it becomes zero. If the leading vehicle is traveling much faster than the following one, the space headway between the two consecutive vehicles will increase and the following vehicle will not brake even though its space headway is smaller than the safety distance. According to Jiang et al. [8], who observed the car-following event, the follower driver's behavior is influenced by the relative velocity between the leading and following vehicles; so, this factor needs to be taken into account. They introduced the full velocity difference (FVD) model, assuming that both positive and negative velocity differences are considered in the following manner

$$\frac{dv_i}{dt} = \kappa(V(\Delta x_i) - v_i) + \lambda \Delta v_i, \tag{7}$$

where $V(\Delta x_i)$ is the optimal velocity function and κ, λ are two reaction coefficients. This model take into account the effects of velocity difference and space headway. But the impact of the driver's attribution on their driving behavior cannot be examined using this model. Based on their attributions, various drivers in a real-world traffic system display varied driving behaviors. Every driver has a different optimal speed and required safety distance. Tang et al. [13] considered the car-following model (8) to account for driver attribution with the optimal speed defined as

$$V(\Delta x_i) = \begin{cases} v_{i-1}(t)\{1 + \tanh(C\,(\Delta x_i(t) - \Delta x_c(t)))\}, \\ \qquad\qquad \text{if } \Delta x_i(t) < \Delta x_c(t), \\ v_{i-1}(t) + (v_{\max} - v_{i-1}(t)) \\ \tanh(C(\Delta x_i(t) - \Delta x_c(t))), \\ \qquad\qquad \text{if } \Delta x_i(t) \geq \Delta x_c(t), \end{cases} \tag{8}$$

where $\Delta x_c(t)$ is an expected space headway connected to the driver's attribution, C is the sensitivity coefficient associated

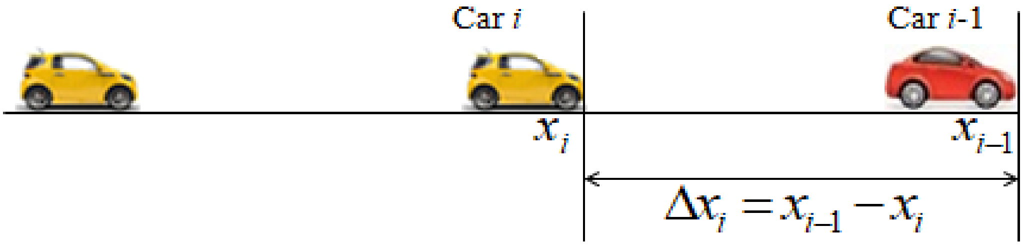

Fig. 2: Schematic diagram of car-following model.

to the safety distance of the driver, and $v_{\max}$ is the maximum speed of the vehicle. The expected headway is defined as

$$\Delta x_c(t) = (1+r)$$

$$\max\left\{h_{c,s}, v_n(t)t_w - \frac{(v_i(t))^2}{2a_{i,\min}} + \frac{(v_{i-1}(t))^2}{2a_{i-1,\min}} + h_{c,s}\right\}, \quad (9)$$

where $h_{c,s}$ represents safety distance of the i^{th} vehicle between the i^{th} and $(i-1)^{th}$ vehicle while stopping the $(i-1)^{th}$ vehicle; t_w is the driver reaction time while stopping the $(i-1)^{th}$ vehicle; $a_{i,min}$ is the maximum deceleration of i^{th} vehicle and r is a parameter showing the attribution of the driver. If $r < 0$ the driver is aggressive, if $r = 0$ the driver is neutral and if $r > 0$ the driver is conservative.

Jiao et al. [9] explored the relation between the vehicle's space headway and optimal velocity, which is expressed as

$$S(\Delta x) = \frac{1}{1 + e^{\Delta x_{\text{safe}} - \mu \Delta x}}, \quad (10)$$

where $S(\Delta x) \in [0,1]$ gives the sensitivity of optimal velocity to the space headway; Δx_{safe} represents the safety space headway; and $0 < \mu < 1$ is a parameter value; $S(\Delta x)$ is the sensitivity of the optimal velocity to the space headway for the different value of parameter μ. The optimal velocity also depends on the speed of the vehicle in front of it as well as on the distance between them. In order to better reflect the peculiarities of the drivers, Jiao et al. [9] proposed a new optimal velocity function, which is expressed as

$$\begin{aligned} V(\Delta x, v_{i-1}) = V_{\max}\left[S(\Delta x) - S(\Delta x_{safe})\right] \\ - \left[1 - S(\Delta x)\right] v_{i-1}(t) \end{aligned} \quad (11)$$

which satisfies the conditions: (i) if $\Delta x = \Delta x_{safe}, V(\Delta x, v_{i-1}) \in [0, v_{i-1}(t)]$, (ii) $\Delta x = \Delta x_{safe}$ and $v_{i-1}(t) = 0, V(\Delta x, v_{i-1}) = 0$, and (iii) if Δx becomes larger, $V(\Delta x, v_{i-1}) \to V_{\max}$. The dynamic equation so-called Reinforcement Car-following (RCF) model [9], which is described as

$$\frac{dv_i(t)}{dt} = \kappa\left[V(\Delta x, v_{i-1}) - v_i(t)\right] + \lambda\,\Delta v. \quad (12)$$

On the basis of the equation (12), it can be observed that when vehicles are closely spaced, the velocity of a following vehicle is primarily influenced by changes in the speed of the leading vehicle. However, as the gap between vehicles increases, the impact of the preceding vehicle's velocity on the following vehicle diminishes. When the distance between vehicles approaches or surpasses a critical threshold, the effect of the leading vehicle's velocity on the following vehicle's diminishes entirely. At this point, the velocity of the following vehicle becomes solely dependent on the maximum speed limit of the road.

C. Vehicle-pedestrian interaction

The pedestrian-vehicle interaction model elucidates the dynamics of pedestrian crossings in the presence of vehicular traffic. A moving vehicle continuously monitors its surroundings for the presence of pedestrians. Immediate braking is initiated by the vehicle upon detecting a pedestrian in close proximity. The vehicle adjusts its speed based on the observed pedestrian activity at the intersection: if pedestrians are present at the intersection, the vehicle decelerates; conversely, if pedestrians remain at the curbside, the vehicle proceeds. Furthermore, pedestrians assess the time required to cross the road compared to the estimated arrival time of approaching vehicles at the intersection. If pedestrians determine that the road can be crossed before the estimated vehicle arrival time, they proceed; otherwise, they await the vehicles' passage at the curbside.

III. Numerical Methods

For the analysis of numerical results, a 5-kilometers-long one way road segment with a width of 10 meters is considered, incorporating non-signalized pedestrian road intersection. The first crossing is located 250 meters from the vehicle generation point, and subsequent crossings are spaced 500 meters apart. A platoon of homogeneous vehicles, spaced 7.4 meters apart, is generated with random initial speeds and controlled using a car-following model. The simulation includes homogeneous groups of light-duty vehicles (LDVs), heavy-duty vehicles (HDVs), passenger cars, petrol vans, and diesel vans. The lead vehicle driver observes pedestrians ahead. The interaction zone is defined as 40 meters before the intersection. If the lead vehicle reaches the interaction zone and pedestrians are present at the intersection, the driver decelerates and brakes when they are within 1 meter. The other vehicles follow the car-following model. In the simulation, pedestrians are considered to arrive at the curbside according to a Poisson distribution, estimating their time to cross. If the pedestrian's crossing time is less than the arrival time of the first vehicle at the intersection, they cross; otherwise, they wait until the last vehicle passes. For numerical simulations, a reinforcement car-following model (12) is employed to handle interactions with pedestrians at intersections. Pedestrian-to-pedestrian interactions are excluded to simplify the simulation. Since the car-following model (12) cannot be solved analytically, the Euler forward difference method is used to discretize the equations of motions into

$$v_i(t+\Delta t) = v_i(t) + \frac{dv_i(t)}{dt}\Delta t, \quad (13)$$

$$x_i(t+\Delta t) = x_i(t) + v_i(t)\Delta t + \frac{1}{2}\frac{dv_i(t)}{dt}(\Delta t)^2, \quad (14)$$

where $\Delta t = 0.01$ is the size of the time step. The study is carried out considering the normal behavior of the driver. The parameters $\lambda = 0.5$, $\Delta x_{\text{safe}} = 7.4\,m, \kappa = 0.41$, $v_{\max} = 14.66\,ms^{-1}$ are adopted from the literature [8]. The other parameter $\mu = 0.07$ is adopted from the literature [9]. The position of pedestrians is updated by laws of motion

$$y_j(t+\Delta t) = y_j(t) + v_j\,\Delta t. \quad (15)$$

The data on emissions and fuel consumption per unit of time are taken from the literature [14] and [15]. The model curve is fitted using the least squares method for vehicular emissions and fuel consumption. The amount of vehicular emissions like NOx, CO, HC and fuel consumption are estimated using this fitted curve over the time against instantaneous speed. Then the fuel consumption rate and emission rate per kilometer of CO, NOx, and HC emitted from the different vehicles against instantaneous speed are estimated. The emissions of all vehicles are calculated, and their average is compared with the data found in the literature. The study focuses on the impact of interaction in the urban areas, so $14.66\,m/s$ is considered as the maximum speed limit for the driving vehicles. The total amount of emission of CO, NOx and CO emitted from each vehicle against their respective instantaneous speed, is calculated using numerical integration. The total amount of fuel consumption of different vehicles is also calculated using the same numerical method.

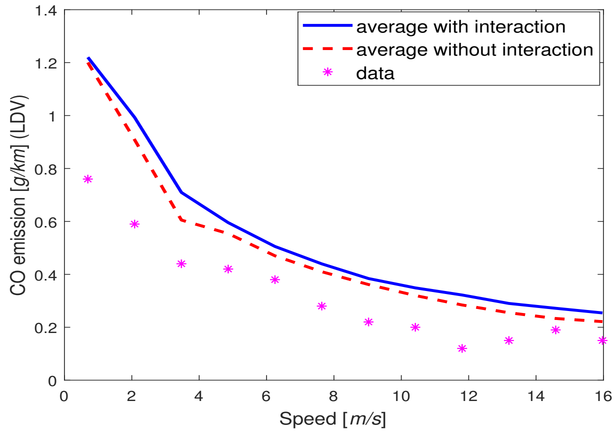

(a) CO emission rate of LDV.

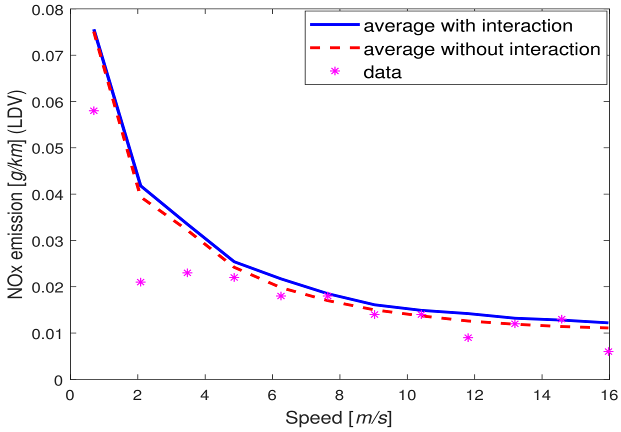

(b) NOx emission rate of LDV.

Fig. 3: CO and NOx emissions rates from LDV.

IV. Results and Discussion

The numerical results have been carried out on the basis of simulation result running the program code for $300s$ using computer programming. The emission and fuel consumption rates are calculated by dividing the total emission and fuel consumption by the distance traveled by each vehicle against the respective instantaneous speed considering interaction and without interaction at the intersection. Similarly, the average emission and fuel consumption of all vehicles have been calculated by averaging the total emission and fuel consumption of all vehicles against instantaneous speed.

The Fig. 3 and Fig. 4 show the emission rate of CO and NOx emitted from the LDVs and HDVs. The Fig. 3a represents the CO emission rate and Fig. 3b represents NOx emission rate per kilometer from LDVs. Similarly, the Fig. 4a represents the CO emission rate and Fig. 4b represents NOx emission rate per kilometer from LDVs. The blue line represents the average emission rate of CO and NOx from LDVs and HDVs which are estimated considering the interaction at the intersection whereas red line represents the emission rate of LDVs and HDVs without considering interaction. It has been observed that there is the impact of intersection in CO and NOx emission due to the interaction with pedestrian at intersection. The average emission rate of CO and NOx is higher than that of average emission rate without interaction. It can be noticed that the emission rate decreases as the instantaneous speed increases. The estimated results are also compared with the real data taken from the literature [15]. The estimated vehicular emissions from LDVs and HDVs are seen to be in agreement with the real data taken from the literature. From these figures, it can be observed that the vehicular emissions have good agreement with data values in higher instantaneous speed rather than in low speed. This may be due to the fact that the emissions are higher with the low speed of the vehicles traveling the short distance. Analyzing the graphs in Fig. 3 and Fig. 4, it can be concluded that the vehicular emission rate of CO and NOx from LDVs and HDVs are higher in the case of interaction with pedestrians at the intersection.

The Fig. 5 represents the average fuel consumption rate and HC emission rate from petrol passenger car against the instantaneous speed. The Fig. 5a represents the average fuel consumption rate per kilometer of the passenger car. The fuel consumption rate of vehicles in slow speed has same rate with and without interaction but fuel consumption is slightly increases of interacting vehicles with increase in instantaneous speed. The fuel consumption pattern matches with the real data taken from the literature [14]. The Fig. 5b represents the average HC emission rate per kilometer of the passenger car. The average HC emission rate per kilometer of petrol passenger car in slow speed has same rate with and without interaction but slightly increases of interacting vehicles at non-signalized intersection with

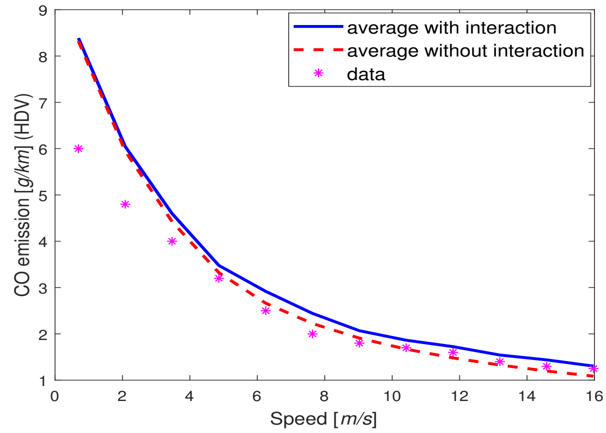

(a) CO emission rate of HDV.

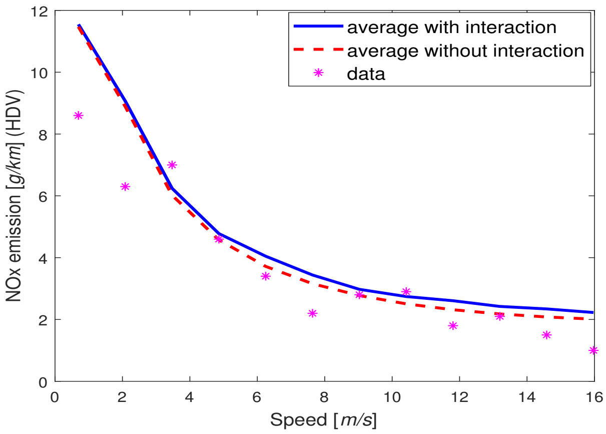

(b) NOx emission rate of HDV.

Fig. 4: CO and NOx emissions rates from HDV.

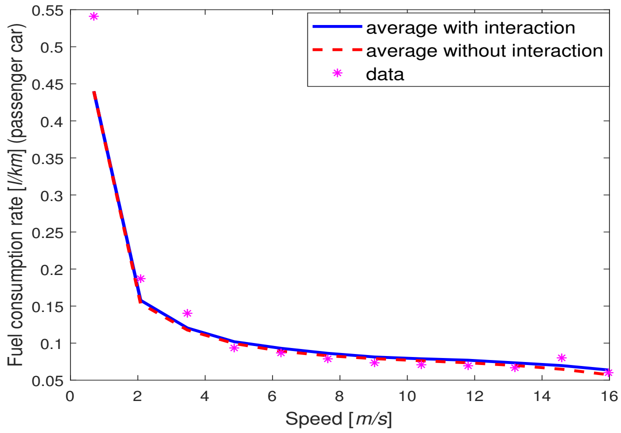

(a) Fuel consumption rate of petrol passenger car.

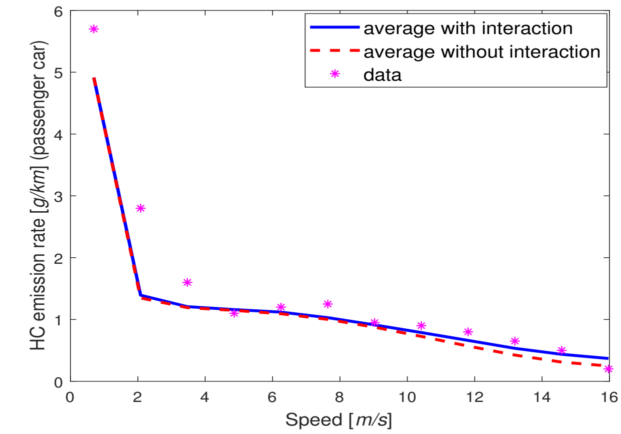

(b) HC emission rate of petrol passenger car.

Fig. 5: Fuel consumption and HC emission from petrol passenger car.

increase in instantaneous speed. The pattern of average fuel consumption and average HC emission from the passenger car seems matched with the real data taken from the previous literature.

The Fig. 6 represents the average fuel emission rate and HC emission rate from petrol van against the instantaneous speed. The Fig. 6a represents the average fuel consumption rate per kilometer of the petrol van. The fuel consumption rate increases for interacting vehicles with increase in instantaneous speed. The fuel consumption pattern matches with the real data taken from the literature [14]. The Fig. 6b represents the average HC emission rate per kilometer of the petrol van.

The Fig. 7 depicts the fuel consumption rate and average emission rate of HC from diesel van with interaction and without interaction at the non-signalized intersection. The Fig. 7a describes the average fuel consumption per kilometer of diesel van and the Fig. 7b represents the average HC emission rate per kilometer from diesel van.

The graphs in the Fig. 8 to Fig. 12 represent the average amount of vehicular emissions and fuel consumption from different types of vehicles. In these figures, the average amount of vehicular emissions and average amount of fuel consumption on running the simulation for 300 s for interacting and non-interacting vehicles at the intersection against instantaneous speed are compared. The graphs in Fig. 8 and Fig. 9 depict the average amount of NOx and CO emitted from LDV and HDV. The Fig. 8a and Fig. 8b represent the average amount of the NOx and CO emitted from the LDVs against instantaneous speed for interacting and non-interacting cases respectively. Though the simulations are conducted for equal time, the average amount of vehicular emission for interacting vehicles seems smaller than the non-interacting case. It is due to the fact that during interaction at the intersection, the vehicles can not be driven long time with its maximum speed as that in non-interacting case. It is due the fact that vehicles cover the fewer distance than that of interacting vehicles and have lower emission rate in low speed.

The Fig. 9a and Fig. 9b respectively represent the average amount of the NOx and CO emitted from the HDVs against instantaneous speed for interacting and non-interacting cases. The average amount of NOx emission in the case of interaction of LDVs is smaller than that of non interacting case because the vehicles in the case of interaction can not cover the distance and can not drive as long as that in the case of non-interaction with its maximum speed. But average amount of CO emission of interacting vehicles against high instantaneous speed is higher than that of

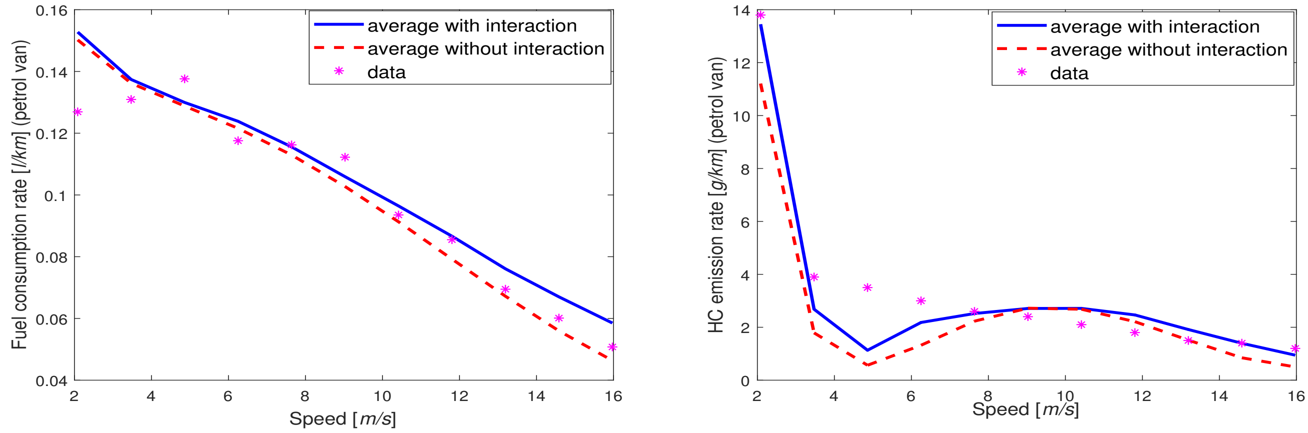

(a) Fuel consumption rate of petrol van.

(b) HC emission rate of petrol van.

Fig. 6: Fuel consumption rate and HC emission rate of petrol van.

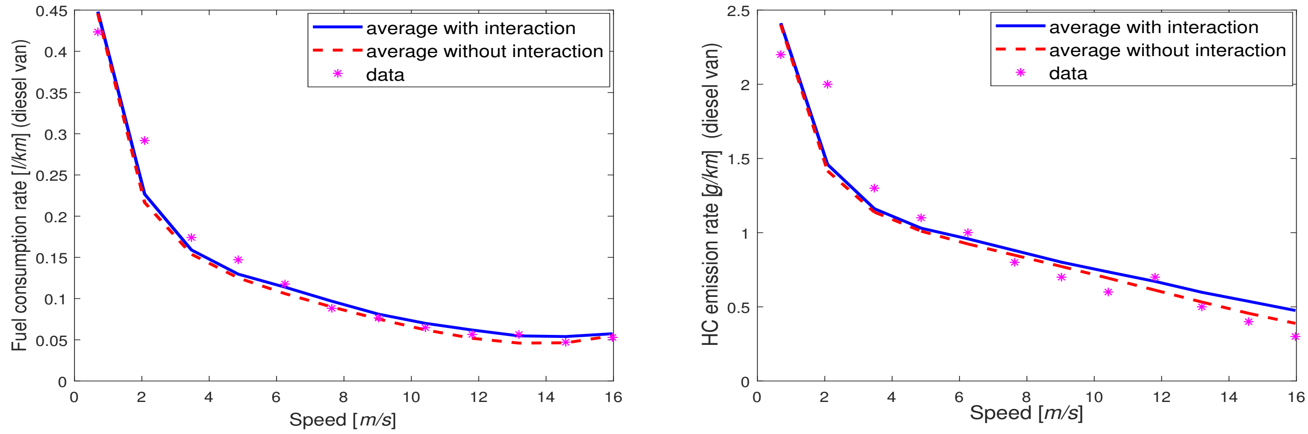

(a) Fuel consumption rate of diesel van.

(b) HC emission rate of diesel van.

Fig. 7: Fuel consumption rate and HC emission rate of diesel van.

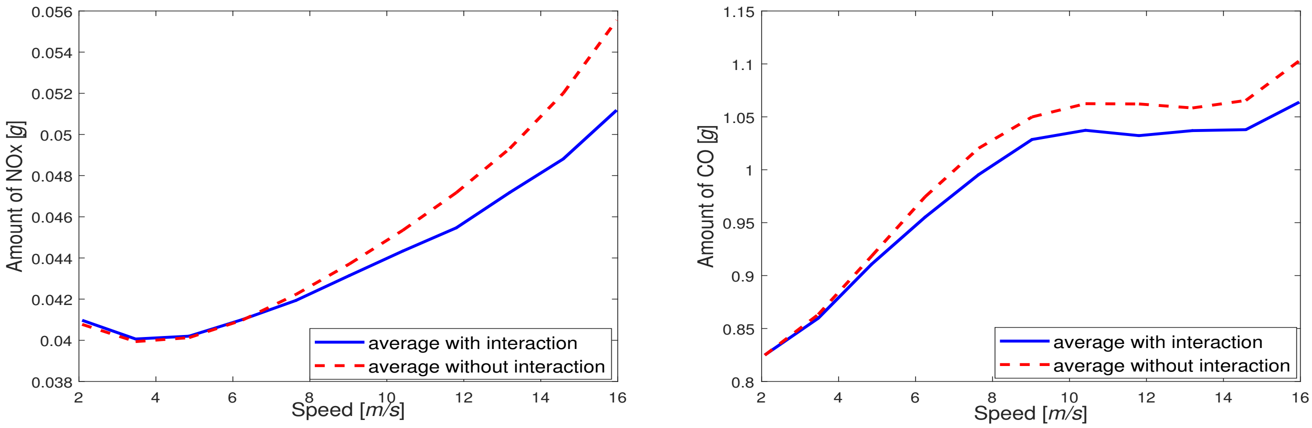

(a) Average amount of NOx emitted from LDV.

(b) Average amount of CO emitted from LDV.

Fig. 8: Average amount of NOx and CO emitted from LDV against instantaneous speed.

non-interacting case.

The graphs in Fig. 10 to Fig. 12 depict the average amount of HC emitted from diesel van, petrol van and petrol passenger car against instantaneous speed. The Fig. 10a represents the average amount of the HC and the Fig. 10b represents the average amount of fuel consumption of the diesel vans against instantaneous speed for interacting and non-interacting cases.

The Fig. 11a and Fig. 11b represent the average amount of the HC and average amount of fuel consumption of the petrol vans respectively against instantaneous speed for

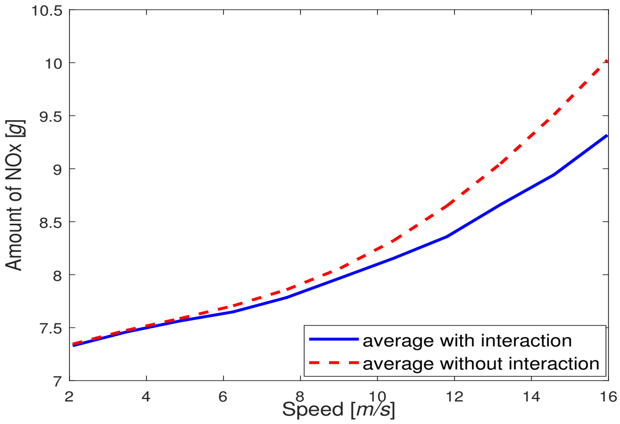

(a) Average amount of NOx emitted from HDV.

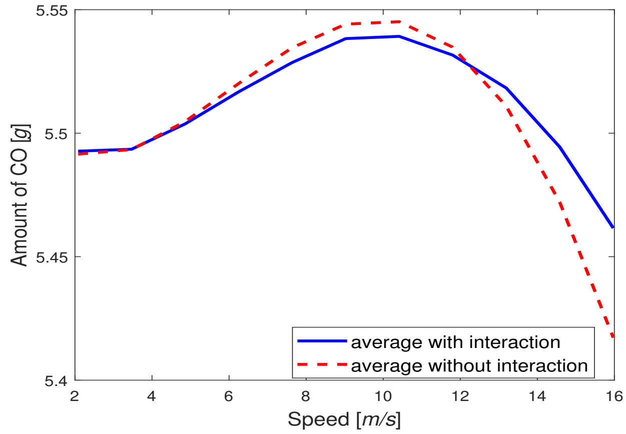

(b) Average amount of CO emitted from HDV.

Fig. 9: Average amount of NOx and CO emission from HDV against instantaneous speed.

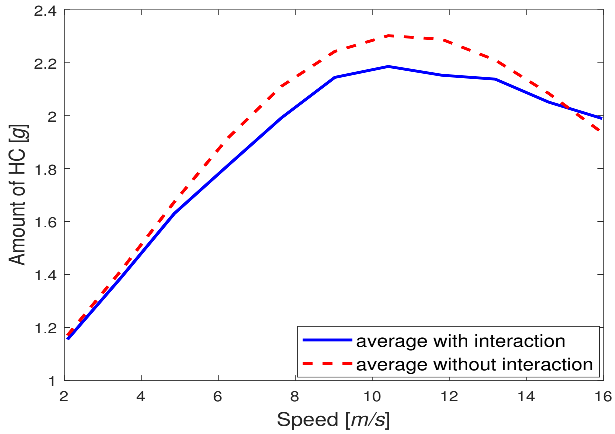

(a) Average amount of HC emission from diesel van.

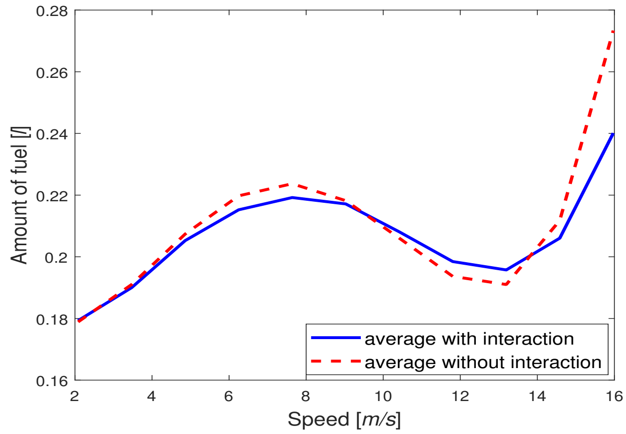

(b) Average amount of fuel consumption of diesel van.

Fig. 10: Average amount of HC and fuel consumption from diesel van against instantaneous speed.

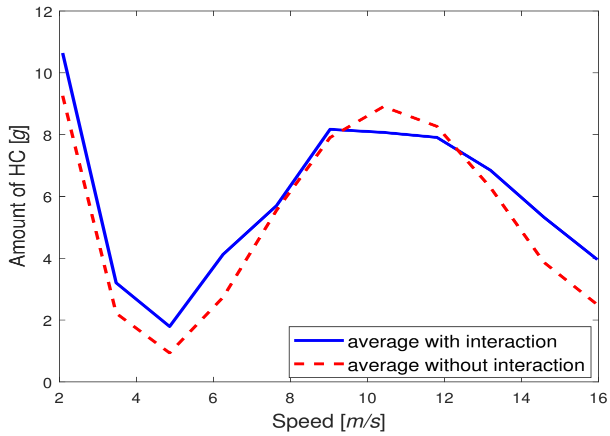

(a) Average amount of HC emission from petrol van.

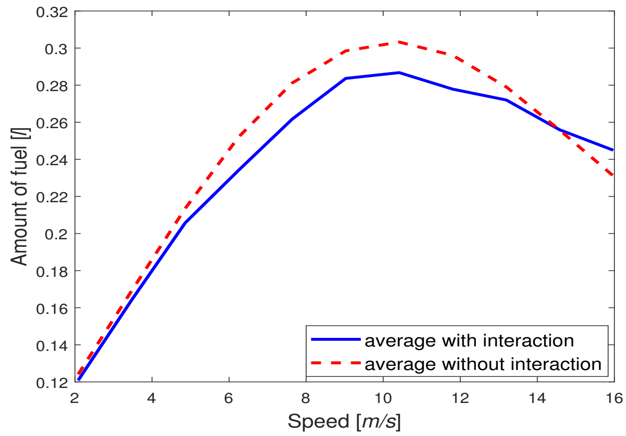

(b) Average amount of fuel consumption of petrol van.

Fig. 11: Average amount of HC emission and fuel consumption from petrol van against instantaneous speed.

interacting and non-interacting cases.

The Fig. 12a and Fig. 12b represent the average amount of the HC and average amount of fuel consumption of the petrol passenger car against instantaneous speed for interacting and non-interacting cases. Analyzing the graphs in Fig. 10 to Fig. 12, the interaction at the intersection impacts in HC emission and fuel consumption of driving vehicles.

V. Conclusion

This study is carried out simulating a platoon of vehicles by considering with and without the interaction at the non-

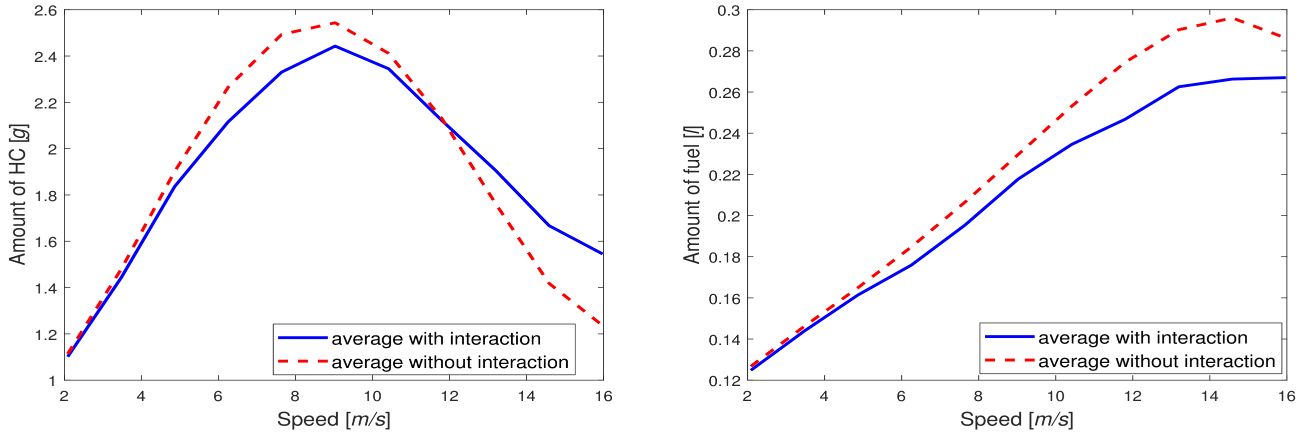

(a) Average amount of HC emission from petrol passenger car.

(b) Average amount of fuel consumption of petrol passenger car.

Fig. 12: Average amount of HC emission and fuel consumption from petrol passenger car against instantaneous speed.

signalized road crossing. The vehicles are moved forward using the car-following models and pedestrian who come at the curb side of the road segment at the intersection following Poisson distribution and cross the road by estimating the road crossing time and vehicle arriving time. The driver of the leading vehicle observes the pedestrians along the road in front and accelerates or decelerates accordingly obeying the car-following model. The vehicular emissions and fuel consumption are fitted by the curve using the data from the literatures by the method of least squares over the time against instantaneous speed. Then average vehicular emission rate, fuel consumption rate per kilometer and average amount of vehicular emission together with fuel consumption are estimated by performing the numerical simulations. From the simulation and analysis of the results, it can be observed that the interaction at the intersection of the road segment has impacted on vehicular emissions and fuel consumption. The amount of vehicular pollutions like NOx, CO, HC etc. depends on how fast or how slow the vehicles are driven. The number of vehicles in a group also contribute to amount of the emission. The crossing behavior of the pedestrian at the interaction may impact on emission and fuel consumption. The frequency of interaction of the vehicles at the intersection, time duration of driving, vehicles type may also impact on vehicular emission and fuel consumption. The attribution of driver of the vehicle have negligible impact on emission and fuel consumption which is not mentioned in the results analysis.

REFERENCES

[1] M. S. Alam, and A. Khan, "The impact study of vehicular pollution on environment," *International Journal for Science and Advance Research in Technology*, vol. 6, no. 12, pp. 30-37, 2020.

[2] M. Bando, K. Hasebe, A. Nakayama, A. Shibata, and Y. Sugiyama, "Dynamical model of traffic congestion and numerical simulation," *Phys. Rev. E,* vol. 51, no. 2, pp. 1035-1042, 1995.

[3] S. Bhandarkar, "Vehicular pollution, their effect on human health and mitigation measures," *Veh. Eng,* vol. 1, no. 2, pp. 33-40, 2013.

[4] S. Dey, and N. S. Mehta, "Automobile pollution control using catalysis," *Resources, Environment and Sustainability*, vol. 2, 2020.

[5] U.S. Environmental Protection Agency, "Vehicle and Fuel Emissions Testing," *https://www.epa.gov/vehicle-and-fuel-emissions-testing*, 2024, Accessed: 2024-08-27.

[6] N. Gartener, "Traffic flow theory: A state-of-the-art report," *URL= http://www. cta. ornl. gov/cta/research/trb/tft. html*, 2001.

[7] D. Helbing, and B. Tilch, "Generalized force model of traffic dynamics," *Phys. Rev. E*, vol. 58, no. 1, pp. 133-138, 1998. doi.10.1103/PhysRevE.58.133.

[8] R. Jiang, Q. S. Wu, and Z. J. Zhu, "Full velocity difference model for a car-following theory," *Phys. Rev. E*, vol. 64, no. 1, 2001.

[9] S. Jiao, S. Zhang, B. Zhou, Z. Zhang, and L. Xue, "An extended car-following model considering the driver's characteristics under a V2V communication environment," *Sustainability*, vol. 12, no. 4, 2020. doi.org/10.3390/su12041552.

[10] X. Li, and J. Sun, "Effect of interactions between vehicles and pedestrians on fuel consumption and emissions," *Physica A: Statistical Mechanics and its Applications*, vol. 416, pp. 661-675, 2014.

[11] O. V. Lozhkina, and V. N. Lozhkin, "Estimation of nitrogen oxides emissions from petrol and diesel passenger cars by means of on-board monitoring: Effect of vehicle speed, vehicle technology, engine type on emission rates," *Transportation Research Part D: Transport and Environment*, vol. 47, pp. 251-264, 2016.

[12] T. Q. Tang, Y. Wang, X. Yang, and Y. Wu, "A new car-following model accounting for varying road condition," *Nonlinear Dynam.*, vol. 70, pp. 1397-1405, 2012.

[13] T. Q. Tang, J. He, S. C. Yanga, and H. Y. Shang, "A car-following model accounting for the driver attribution," *Physica A*, vol. 413, pp. 583-591, 2014.

[14] H. Y. Tong , W. T. Hung, and C. S. Cheung, "On-Road Motor Vehicle Emissions and Fuel Consumption in Urban Driving Conditions," *Journal of the Air & Waste Management Association*, vol. 50, no. 4, pp. 543-554, 2000.

[15] Shengli Wei, Tongyuan Ding, Shupei zhang, Ping Tao, and Jie Chen, "Analysis of vehicle CO and NOx road emissions test based on PEMS," *Energy Sources, Part A: Recovery, Utilization, and Environmental Effects*, pp. 1-15, 2020.